Q factor: A measure of competition between the topper and the average in percolation and in self-organized criticality

Asim Ghosh,[1,*] S. S. Manna[2,†] and Bikas K. Chakrabarti[3,4,‡]
[1]*Department of Physics, Raghunathpur College, Raghunathpur 723133, India*
[2]*B-1/16 East Enclave Housing, 02 Biswa Bangla Sarani, New Town, Kolkata 700163, India*
[3]*Saha Institute of Nuclear Physics, Kolkata 700064, India*
[4]*Economic Research Unit, Indian Statistical Institute, Kolkata 700108, India*

(Received 12 February 2024; revised 15 May 2024; accepted 8 July 2024; published 19 July 2024)

We define the Q factor in the percolation problem as the quotient of the size of the largest cluster and the average size of all clusters. As the occupation probability p is increased, the Q factor for the system size L grows systematically to its maximum value $Q_{\max}(L)$ at a specific value $p_{\max}(L)$ and then gradually decays. Our numerical study of site percolation problems on the square, triangular, and simple cubic lattices exhibits that the asymptotic values of $p_{\max}$, though close, are distinct from the corresponding percolation thresholds of these lattices. We also show, using scaling analysis, that at $p_{\max}$ the value of $Q_{\max}(L)$ diverges as L^d (d denoting the dimension of the lattice) as the system size approaches its asymptotic limit. We further extend this idea to nonequilibrium systems such as the sandpile model of self-organized criticality. Here the $Q(\rho, L)$ factor is the quotient of the size of the largest avalanche and the cumulative average of the sizes of all the avalanches, with ρ the drop density of the driving mechanism. This study was prompted by some observations in sociophysics.

DOI: 10.1103/PhysRevE.110.014131

I. INTRODUCTION

Critical fluctuations of all length scales appearing at the critical points are the signatures of phase transitions. Over the past century, extensive studies of phase transitions have helped establish the statistical-physics descriptions of the scaling theory and the critical phenomena in different physical systems. For example, few well-studied systems are magnetic and fluid systems [1], polymer systems [2,3], percolating systems [3], and self-organized critical (SOC) systems [4]. Essentially, the order parameter of the corresponding systems vanishes following in general a singular power law or critical behavior at the critical point and beyond. Its higher moments include susceptibilities and diverge again with singular or critical power-law exponent values at the respective critical points. For SOC systems, these singular behaviors are seen from the precritical side and then remain critical in the SOC state of the systems. For practical purposes, these diverging susceptibilities help locate the critical point.

For social systems, scientists have studied for ages, starting with Pareto's 80-20 principle [5], the Lorenz function [6], the Gini index [7], the Hirsch index [8], etc., the extreme unequal distributions of income or wealth, votes, and paper citations. Following more recent observations [9–11] of the extreme inequality level in citation statistics of successful individuals and even institutions, universities, and journals, with Gini and other inequality index values going beyond the Pareto 80-20 limit, we studied and found [12] the clear presence of a similar level of inequality index values in the physical models of SOC system, like the Bak-Tang-Wiesenfeld (BTW) sandpile [13] and the Manna [14] sandpile. In particular, in our recent study [15] of citation statistics of some very successful prize-winning scientists and a few other not so successful scientists it was observed that their research dynamics is clearly SOC-like and the most successful achieved the critical level in their citation inequalities, while others were still approaching that level, though they had not reached it. All these studies showed that just the average high level of citations per paper (reflected by the Hirsch index values, which are determined by the effective network coordination or Dunbar number [16,17]), does not reflect the success of the scientist but rather the high level (beyond the Pareto level) of critical fluctuations in citations from publication to publication of the scientist. Indeed, it was seen in [15] that crossing a threshold value of a simple quotient of the citation number of the highest cited paper and the average citation of all the papers (including the highest cited one) by the scientist indicates a very good correlation with the appreciation by the respective communities.

Following this clue, we study here how the topper competes with the average in the well-known models of percolation processes and in the sandpile model of self-organized criticality. In the percolation model we define the Q factor as the quotient of the largest cluster size and the average size over all clusters for the percolation models. Similarly, the Q factor in the sandpile model is defined as the quotient of the largest avalanche size and the average size over all avalanches. As the control variables are tuned in these problems, Q factors grow very sharply right before a specific value of the control variable, reach the maxima, and then decay very rapidly. The

*Contact author: asimghosh066@gmail.com
†Contact author: subhrangshu.manna@gmail.com
‡Contact author: bikask.chakrabarti@saha.ac.in

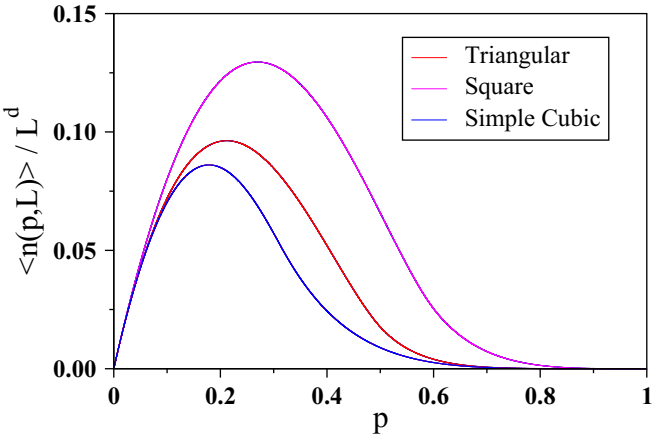

FIG. 1. Plot of the average number of distinct clusters per lattice site $\langle n(p,L)\rangle/L^d$ against the site percolation occupation probability p. For each type of lattice, the data for three different system sizes are plotted and overlap completely; only the colors used for the largest lattices are visible.

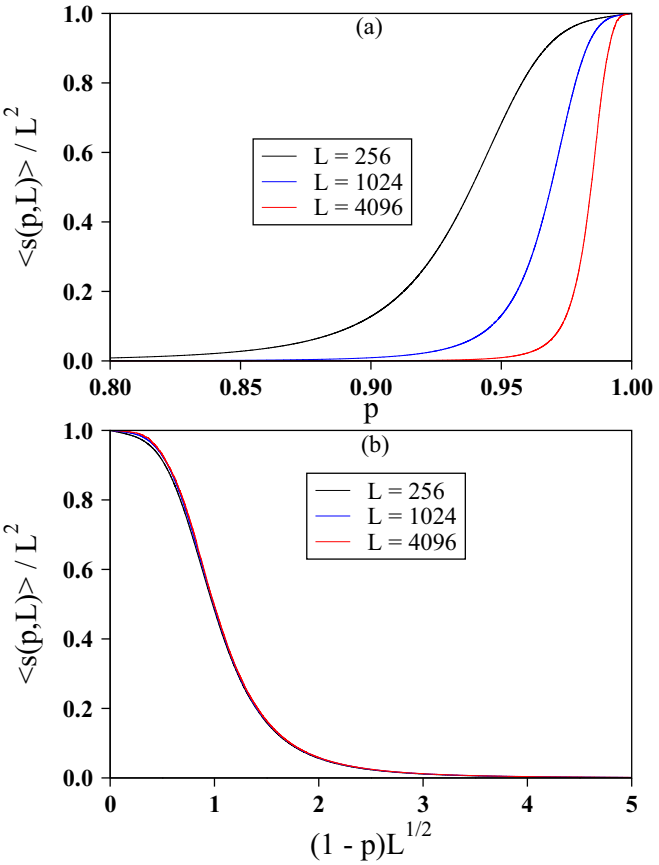

FIG. 2. (a) Plot of the average cluster size $\langle s(p,L)\rangle$ scaled by the total number L^2 of lattice sites against the site percolation occupation probability p for the square lattice. (b) Same data as in (a) plotted against $(1-p)L^{1/2}$, which yields nice collapse of the data.

locations of the maxima are distinct from the critical points of these systems.

In Sec. II we describe our calculations and results of the percolation problem for the square, triangular, and simple cubic lattices. We calculate the Q factors for the entire range of occupation probability p. A nice finite-size extrapolation gives the precise value of the percolation occupation probability $p_{\max}$ in the asymptotic limit, which we find to be larger than their percolation thresholds. In Sec. III we execute a similar analysis for the BTW sandpile where we use the drop density ρ as the tuning parameter. The value of $\rho_{\max}$ in the asymptotic limit is calculated. We summarize in Sec. IV.

II. SITE PERCOLATION

A. Square lattice

An initially empty square lattice of size $L \times L$ is gradually filled in by occupying the randomly selected lattice sites one by one. At any arbitrary intermediate stage the fraction p of occupied sites is referred to as the percolation occupation probability. A cluster is defined as a set of occupied sites connected by nearest-neighbor distances. Different distinct clusters are identified using the well-known Hoshen-Kopelman algorithm [18]. Since we are not going to study any spanning property of the percolation clusters, we use periodic boundary conditions in all simulations reported here. The number of distinct clusters $n(p,L)$ increases from unity at $p \to 0+$, reaches a maximum at some intermediate p value, and then finally goes down to unity again at $p = 1$. We refer to the entire process as a run.

In Fig. 1 we plot the average number of distinct clusters per lattice site $\langle n(p,L)\rangle/L^d$ against p for three different system sizes of the square, triangular, and simple cubic lattices, where d represents the Euclidean dimension of these lattices. The collapse of the plots on top of one another for three system sizes is extremely good. The sizes of the lattices used are $L =$ 256, 1024, and 4096 for the square and triangular lattices and $L = 32$, 64, and 128 for the simple cubic lattice. The peak positions of these curves have coordinates (0.269 68, 0.129 54) for the square lattice, (0.211 92, 0.096 306) for the triangular lattice, and (0.178 71, 0.086 066) for the simple cubic lattice.

At an intermediate stage the average size of all clusters including the largest one is therefore $s_{\rm av}(p,L) = pL^d/n(p,L)$. This is further averaged over a large number of independent runs and we define the average cluster size $\langle s(p,L)\rangle = \langle s_{\rm av}(p,L)\rangle$. In Fig. 2(a) we plot the scaled average cluster size $\langle s(p,L)\rangle/L^2$ against p only for the square lattice and again for the same three system sizes. The curves become sharper as $p \to 1$ and as the system size becomes larger. In Fig. 2(b) the x axis is inverted and the same data $\langle s(p,L)\rangle/L^2$ are plotted against $(1-p)L^{1/2}$ to observe a nice collapse of the data over the entire range of p values.

As more and more sites are occupied, the growth of the size $s_{\max}$ of the largest cluster is monitored. The order parameter $\Omega(p,L)$ of the percolation transition is defined as the fractional size of the largest cluster averaged over many independent runs, i.e., $\Omega(p,L) = \langle s_{\max}(p,L)\rangle/L^d$. In Fig. 3 we plot the order parameter $\Omega_{\rm sq}(p,L)$ for the square lattice for three different system sizes. For a larger system size, the growth of the order parameter becomes sharper. For a particular system $\Omega_{\rm sq}(p,L)$ grows rapidly as the percolation occupation probability p approaches from below the site

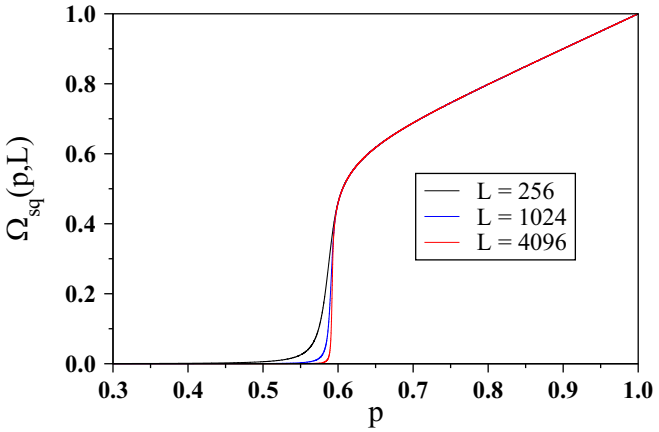

FIG. 3. Plot of the percolation order parameter $\Omega_{\rm sq}(p, L) = \langle s_{\rm max}(p, L)\rangle/L^2$ against the site percolation occupation probability p for the square lattice.

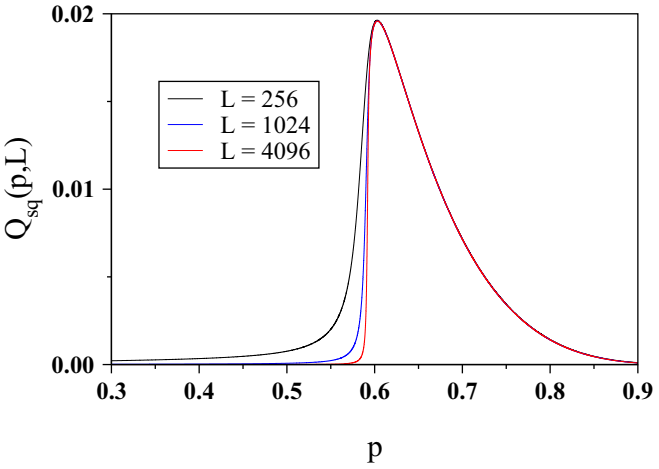

FIG. 5. Plot of $Q_{\rm sq}(p, L)$ against the percolation occupation probability p for the square lattice.

percolation threshold of the square lattice, whose best value to date is $p_c(\text{sq}) = 0.592\,746\,050\,792\,10(2)$ [19,20].

Now we define the Q factor as the quotient of the average size $\langle s_{\rm max}(p, L)\rangle$ of the largest cluster and the average size $\langle s(p, L)\rangle$ of all clusters for every value of p for a certain system size L as

$$Q(p, L) = [\langle s_{\rm max}(p, L)\rangle/\langle s(p, L)\rangle]/L^d = \Omega(p, L)/\langle s(p, L)\rangle. \quad (1)$$

We plot in Fig. 4 three quantities for a particular system size $L = 256$. They are (i) the average size $\langle s_{\rm max}(p, L)\rangle$ of the largest cluster, (ii) the average size $\langle s(p, L)\rangle$ of all clusters, and (iii) the $Q(p, L)$ factor multiplied by the system size L^2. The first two quantities are monotonically increasing functions of p. It is observed that when p gradually increases to a specific value $\langle p_{\rm max}(L)\rangle$, the value of $\langle s_{\rm max}(p, L)\rangle$ becomes increasingly larger than the average cluster size $\langle s(p, L)\rangle$ and therefore $Q(p, L)$ increases very sharply. However,

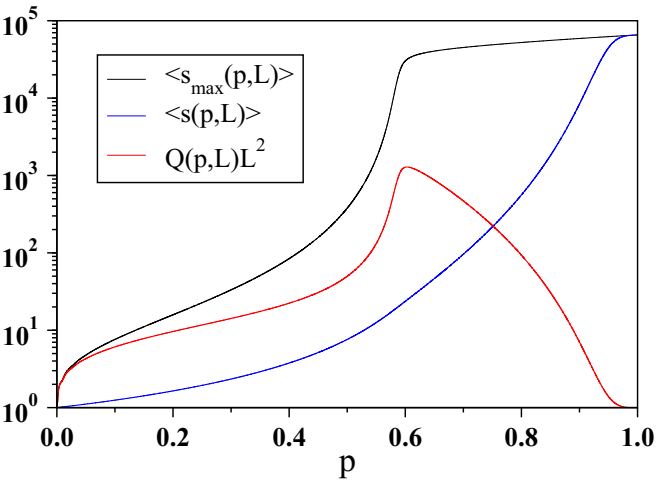

FIG. 4. Plot of the average size of the largest cluster $\langle s_{\rm max}(p, L)\rangle$, average size of all clusters $\langle s(p, L)\rangle$, and Q factor $Q(p, L)L^2$ against the site occupation probability p for a system of size $L = 256$ on the square lattice.

after crossing $\langle p_{\rm max}(L)\rangle$, the growth of $\langle s_{\rm max}(p, L)\rangle$ becomes slower but $\langle s(p, L)\rangle$ maintains its previous growth rate. Consequently, their ratio Q factor decays gradually, which explains the existence of a peak of Q at $\langle p_{\rm max}(L)\rangle$. This is visible in Fig. 5, where $Q_{\rm sq}(p, L)$ is plotted against p for three different system sizes. All three curves have single peaks of nearly the same heights, but their positions have systematic variations.

Now we present numerical evidence in Fig. 6 to claim that the asymptotic value $p_{\rm max} = \lim_{L\to\infty}\langle p_{\rm max}(L)\rangle$ is distinct from the ordinary percolation threshold p_c on the same lattice. Let us denote a typical run from an empty lattice ($p = 0$) to a fully occupied lattice ($p = 1$) on a square lattice of size $L \times L$ by α. For every α we estimate three different values of the occupation probability, namely, (i) the value of occupation probability $p_c(\alpha, L)$ at which the occupation of only the next site in the sequence causes the maximal jump of the size of the largest cluster $s_{\rm max}(\alpha, L)$, (ii) the value of $p_Q(\alpha, L)$ at which the occupation of only the next site in the sequence causes the maximal jump of the value of the $Q(\alpha, L)$ factor, and (iii) the value of $p_{\rm max}(\alpha, L)$ at which the ratio $s_{\rm max}(\alpha, p, L)/s_{\rm av}(\alpha, p, L)$ reaches its maximum value.

Their average values $\langle p_c(L)\rangle$, $\langle p_Q(L)\rangle$, and $\langle p_{\rm max}(L)\rangle$ have been calculated over a large number of runs, namely, 10^8 runs for lattices of size up to $L = 128$, which decreases to 18 000 for $L = 4096$. Each of these quantities is then extrapolated using a finite-size correction term in the power-law form $\langle p_c(L)\rangle = p_c - AL^{-1/\nu_k}$, where ν_1, ν_2, and ν_3 correspond to p_c, p_Q, and $p_{\rm max}$, respectively. Here $\nu_1 = \nu$ is the ordinary correlation length exponent of the two-dimensional percolation problem. In comparison to $1/\nu_1 = 0.75$, we get 0.7574, which is quite close. The values of $1/\nu_2 = 0.9145$ and $1/\nu_3 = 1.0425$ show that the values of ν_2 and ν_3 are quite different from ν, but their values are close to each other and nearly equal to 1.

After extrapolation, the asymptotic value of $p_c = 0.592\,717$ is obtained, which is very close to the actual value of the site percolation threshold approximately equal to 0.592 746, with a difference of approximately 0.000 03.

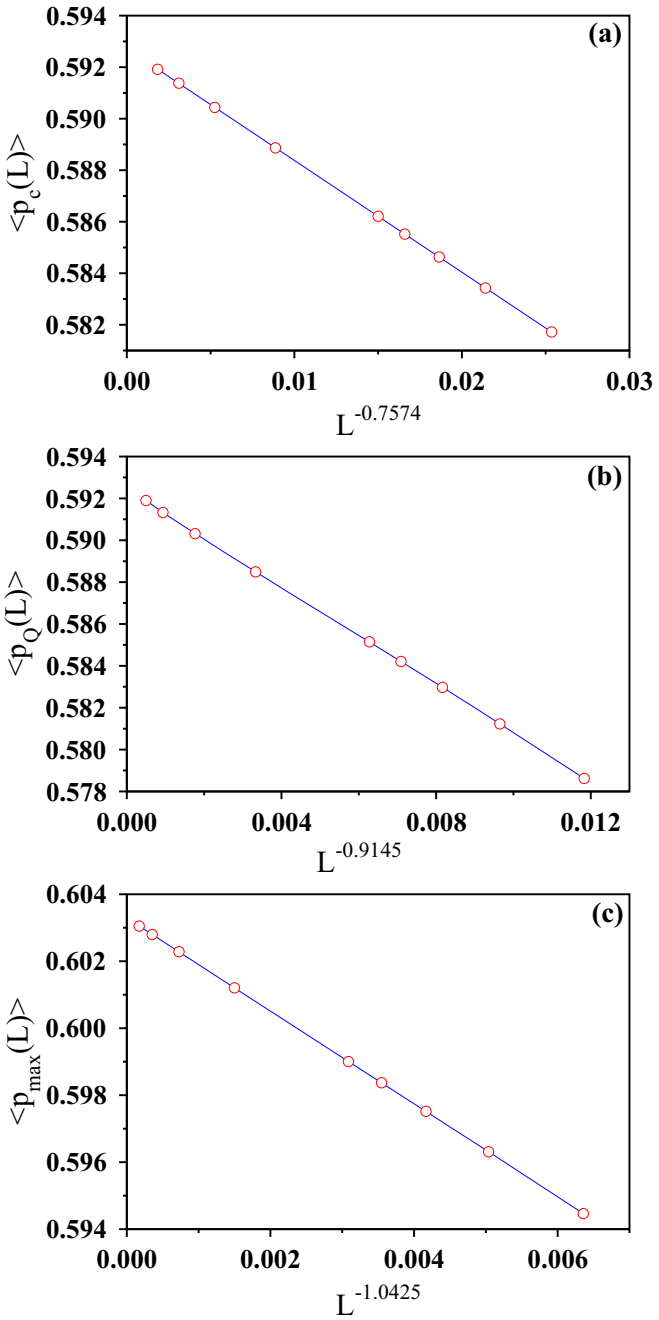

FIG. 6. Finite-size extrapolations with suitable tuning parameters yield (a) $p_c = 0.592\,717$ and $1/\nu_1 = 0.7574$, (b) $p_Q = 0.592\,419$ and $1/\nu_2 = 0.9145$, and (c) $p_{\max} = 0.603\,288$ and $1/\nu_3 = 1.0425$.

The asymptotic value of $p_Q = 0.592\,419$ is found, which is approximately equal to 0.0003 away from the percolation threshold, whereas the asymptotic value of $p_{\max} = 0.603\,288$ differs from the percolation threshold by an amount approximately equal to 0.01. With this analysis, we conclude that while the values of p_Q and p_c are most likely to be the same, the value of $p_{\max}$ is in fact distinct from p_c.

In the following analysis we calculate and plot the ratios of successive values of three quantities. Specifically, if the occupation probability is increased by a small amount of, say, $\Delta p = 1/L^2$, i.e., one more site is occupied, then to what factors are the quantities (i) $\langle s_{\max}(p, L)\rangle$, (ii) $\langle s(p, L)\rangle$, and (iii) $Q(p, L)$ increased? These ratios are defined as

$$\mathcal{R}[\langle s_{\max}(p, L)\rangle] = \frac{\langle s_{\max}(p + \Delta p, L)\rangle}{\langle s_{\max}(p, L)\rangle},$$

$$\mathcal{R}[\langle s(p, L)\rangle] = \frac{\langle s(p + \Delta p, L)\rangle}{\langle s(p, L)\rangle},$$

$$\mathcal{R}[Q(p, L)] = \frac{\langle Q(p + \Delta p, L)\rangle}{\langle Q(p, L)\rangle} = \frac{\mathcal{R}[\langle s_{\max}(p, L)\rangle]}{\mathcal{R}[\langle s(p, L)\rangle]},$$

respectively, and are plotted in Fig. 7 for $L = 256$. In Fig. 3 we find that the size of the largest cluster increases very fast right before the percolation threshold, but right after percolation it starts increasing with p approximately linearly. Therefore, $\mathcal{R}[\langle s_{\max}(p, L)\rangle]$ must have a peak at $p_c(L)$, and the black curve indeed shows a peak at $p_c(L = 256) \approx 0.579\,815$. From Fig. 2 we observe that the value of $\langle s(p, L)\rangle$ increases very slowly except when p is nearly equal to 1. Therefore, the red curve in Fig. 7 exhibits the slow variation of $\mathcal{R}[\langle s(p, L)\rangle]$ against p. Consequently, their ratio $\mathcal{R}[Q(p, L)]$ (in blue) also has a peak at p_c, and beyond this peak, it decreases systematically.

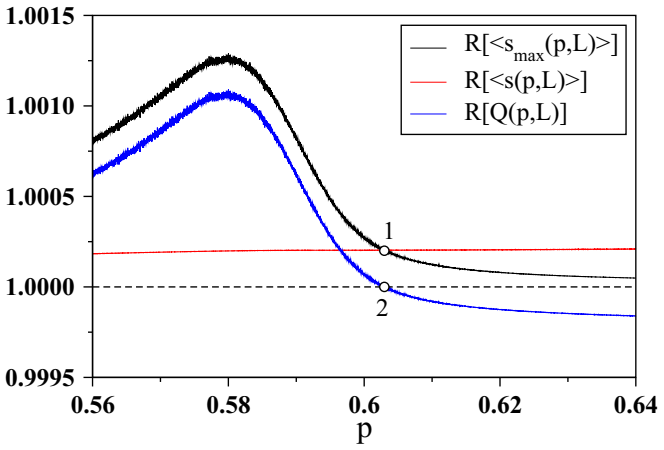

FIG. 7. Plot of $\mathcal{R}[\langle s_{\max}(p, L)\rangle]$, $\mathcal{R}[\langle s(p, L)\rangle]$, and $\mathcal{R}[Q(p, L)]$ against the site occupation probability p for the square lattice of size $L = 256$. The first two curves meet at point 1, where their values are equal. Therefore, their ratio is unity, which corresponds to $\mathcal{R}[Q(p, L)] = 1$ at point 2.

Two points should be noticed. The Q factor has its maximum at $p_{\max}(L)$ where the ratio $\mathcal{R}[Q(p, L)]$ is equal to unity. Therefore, at $p = p_{\max}(L)$ the two curves meet at point 1 where $\mathcal{R}[\langle s_{\max}(p, L)\rangle] = \mathcal{R}[\langle s_{\rm av}(p, L)\rangle]$. Point 2 on the plot of $\mathcal{R}[Q(p, L)]$ against p represents the point $\mathcal{R}[Q(p_{\max}, L) = 1]$. We argue that $p_c(L)$ and $p_{\max}(L)$ both assuming the same asymptotic value, i.e., $p_c = p_{\max}$, would mean a discontinuous drop in the value of $\mathcal{R}[Q(p)]$ at this value of p, which is not possible since both the largest and the average cluster sizes vary continuously in a continuous phase transition like the ordinary percolation.

We have calculated the error in our estimate for the asymptotic value of $p_{\max}$. For a system of size L we have calculated the standard deviation $\sigma(L) = [\langle p^2_{\max}(L)\rangle - \langle p_{\max}(L)\rangle^2]^{1/2}$.

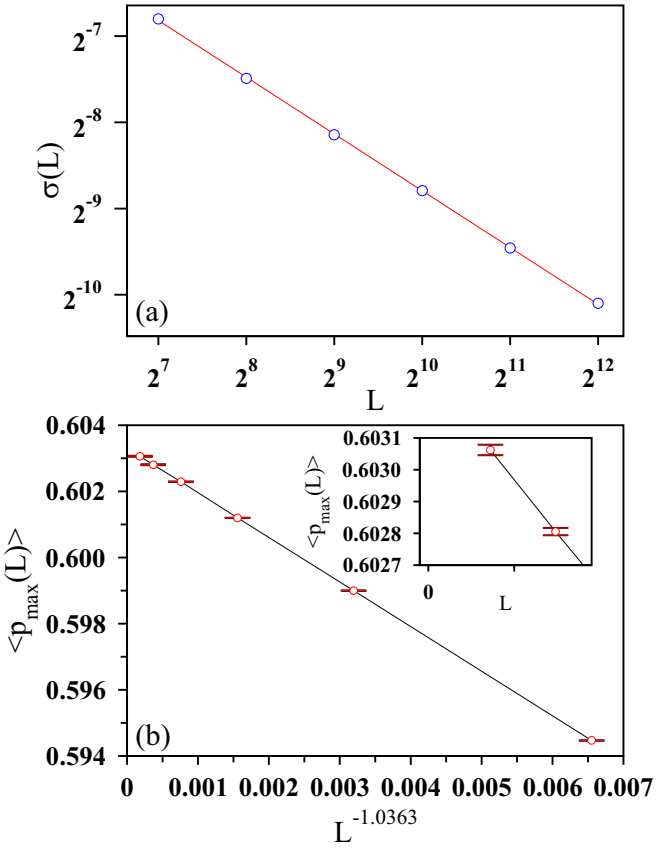

FIG. 8. (a) Plot of the standard deviation $\sigma(L)$ for the values of $p_{\max}(L)$ of the square lattice against the system size L on a log-log scale. The estimation of slope implies $\sigma(L) \sim L^{-0.658}$. (b) Plot of the average values of $\langle p_{\max}(L)\rangle$ against $L^{-1.0363}$ to obtain a nice straight line. Each point is marked with its error bar. The extrapolated value of $p_{\max} = 0.6033 \pm 0.0002$ has been obtained.

In Fig. 8(a) the values of $\sigma(L)$ are plotted against L using a double-logarithmic scale. We observe that $\sigma(L)$ nicely scales as $L^{-0.658}$. Denoting the number of independent runs be M, we define the error as $e(L) = \sigma(L)/M^{1/2}$. For this plot the number of runs M varies from 24×10^6 for $L = 128$ to 3000 for $L = 4096$. In Fig. 8(b) the values of $\langle p_{\max}(L)\rangle$ are plotted against $L^{-1.0363}$, as well as errors using the vertical lines. For each point we have drawn a vertical line from $\langle p_{\max}(L)\rangle - e(L)$ to $\langle p_{\max}(L)\rangle + e(L)$ and then two horizontal bars of fixed length at the two ends of the vertical line (a close-up of only the two points for $L = 2048$ and 4096 is shown in the inset for clarity). It is obvious that the errors are really small. We conclude that the maximal error in the estimation of the asymptotic value of $p_{\max}$ quite possibly is 0.0002 and therefore our final estimate is $p_{\max} = 0.6033 \pm 0.0002$, which is distinct from the actual value of $p_c \approx 0.592\,746$.

We also try a logarithmic correction to the finite-size correction as follows:

$$\langle p_{\max}(L)\rangle = p_{\max} - AL^{-\alpha}[1 - B(\ln L/L)]. \tag{2}$$

From our best fit we obtain $p_{\max} = 0.60329$, $A = 1.4323$, $\alpha = 1.047$, and $B = 0.2608$, which shows that the logarithmic correction has very little effect on $p_{\max}$ (figure not shown).

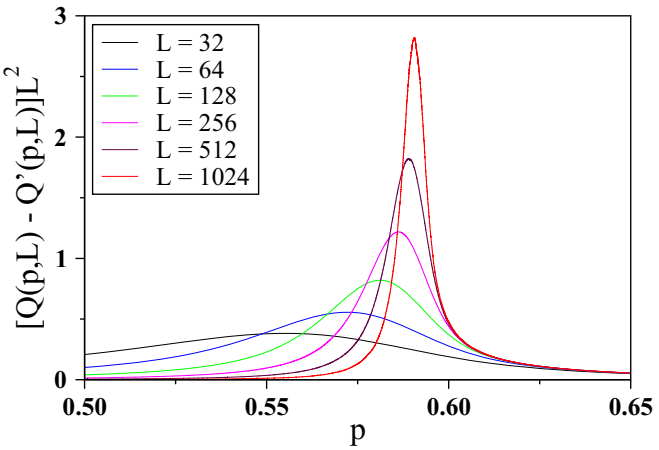

FIG. 9. Plot of the difference $\Delta Q = [Q(p, L) - Q'(p, L)]L^2$ for six different sizes of the square lattice against the site occupation probability p.

The collapse of the peak positions $Q_{\max}(p_{\max}, L)$ of the curves in Fig. 5 on one another implies the maximal cluster size at this point $\langle s_{\max}(L)\rangle \sim L^{\eta}$, with $\eta = 2$. This is directly verified by plotting (figure not shown) $\langle s_{\max}(L)\rangle$ against L using double-logarithmic scales for the square and simple cubic lattices. The values of the exponent η are estimated from the slopes of the curves. For the square lattice $\eta_{\text{sq}} = 2.0057$ is obtained and for the simple cubic lattice $\eta_{\text{sc}} = 3.0075$ is found. This implies that since the $\langle p_{\max}\rangle$ values are slightly larger than the percolation thresholds, the largest clusters turn out to be compact, and not fractals like the percolating clusters at the percolation thresholds. Consequently, their dimensions are equal to their embedding space dimensions. This analysis gives further support to our claim that p_c and $p_{\max}$ are indeed distinct from each other.

An alternate definition of the Q factor is as follows:

$$Q'(p, L) = \langle [s_{\max}(p, L)/s_{\text{av}}(p, L)]\rangle / L^d. \tag{3}$$

Here, for each value of p of every run, we first calculate the quotient of the largest cluster size $s_{\max}(p, L)$ and the average cluster size $s_{\text{av}}(p, L)$ and then take an average of this quotient over a large number of independent runs.

We calculate both the $Q(p, L)$ and $Q'(p, L)$ factors for the same set of runs. When we plot these two Q factors against p on the same graph, it appears to the naked eye that one curve completely overlaps the other as if the two factors were equal. Actually, this is not the case, which becomes apparent when we plot the difference $\Delta Q = [Q(p, L) - Q'(p, L)]L^2$ against p in Fig. 9 for six different sizes of the square lattice. It is observed that though the maximal value of the difference is very small, there is a nice peak for ΔQ occurring at $\langle p_{\max}(L)\rangle$. The number of independent runs varies from 10^8 up to $L = 64$ to 320 000 for $L = 1024$. The locations of the maxima, i.e., $p_{\max}$ and $p'_{\max}$ for $Q(p, L)$ and $Q'(p, L)$, respectively, are almost always the same; if not, they differ by an amount of approximately equal to $1/L^2$. They are extrapolated as $\langle p_{\max}(L)\rangle = 0.603\,312 - \text{const} \times L^{-2.1429}$.

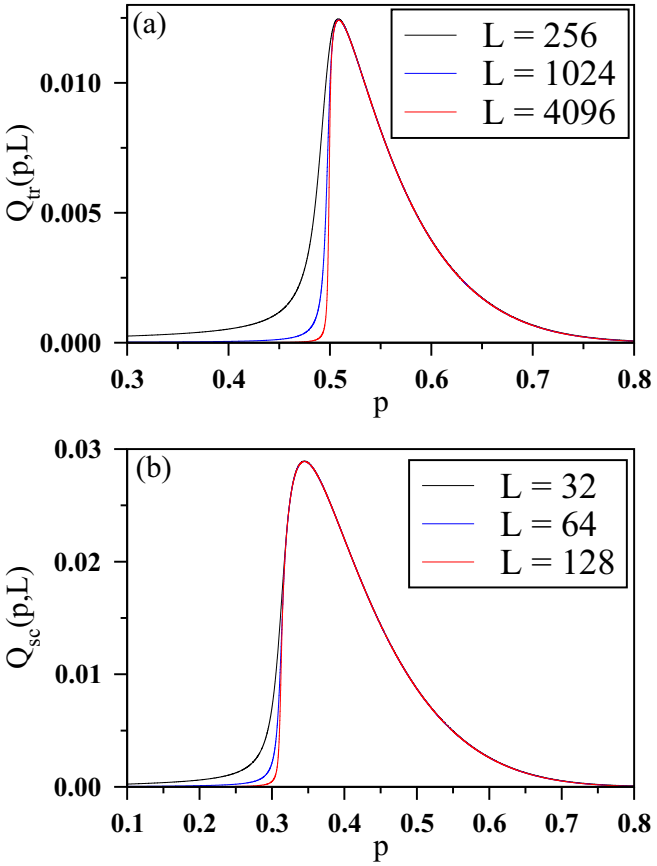

FIG. 10. Plot of the Q factors against the site occupation probability p for two different lattices: (a) $Q_{\rm tr}(p, L)$ for the triangular lattice and (b) $Q_{\rm sc}(p, L)$ for the simple cubic lattice.

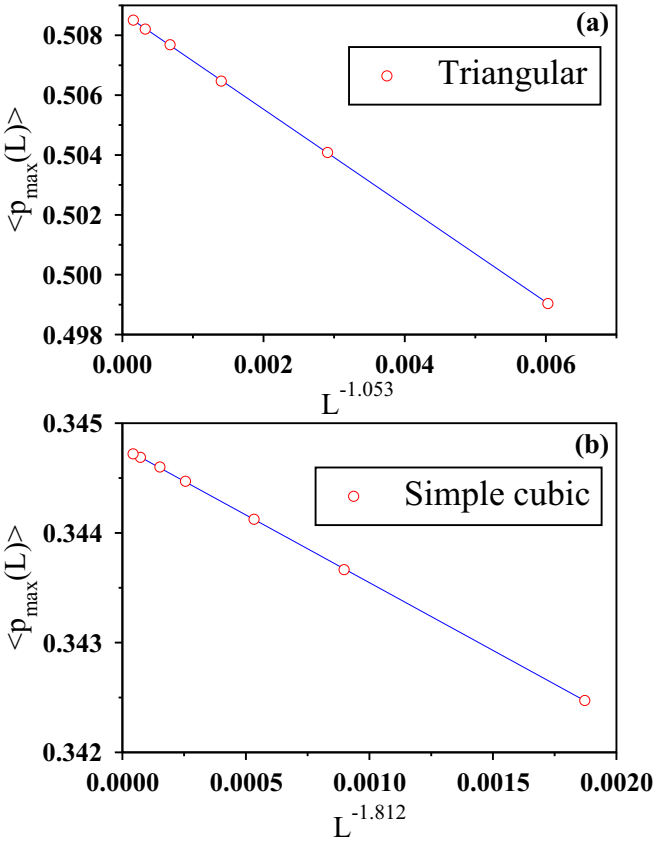

FIG. 11. Extrapolation of $\langle p_{\rm max}(L)\rangle$ values to their asymptotic limit of $L \to \infty$ gives the estimates of $p_{\rm max}$: (a) 0.5088 for the triangular lattice and (b) 0.3448 for the simple cubic lattice.

B. Triangular lattice

A parallel set of calculations is done on the triangular lattice. A plot of $Q_{\rm tr}(p, L)$ against p for three different system sizes is shown in Fig. 10(a). The positions of the maxima are very close to the triangular lattice percolation threshold $p_c = 1/2$ but slightly larger than 1/2. For each run we estimate the maximum value of $Q_{\rm max}(p_{\rm max}, L)$ and the corresponding $p_{\rm max}$ values and then average over all runs. The average $\langle p_{\rm max}(L)\rangle$ values of six different system sizes for $L = 128, \ldots, 4096$ are extrapolated to their asymptotic limit $\langle p_{\rm max}(L)\rangle = p_{\rm max} - \text{const} \times L^{-1.053}$, with $p_{\rm max} = 0.5088$, which is approximately 0.9% different from the percolation threshold $p_c = 1/2$ [see Fig. 11(a)].

C. Simple cubic lattice

For the simple cubic lattice we could study only small lattice sizes up to $L = 256$ which are plotted in Fig. 10(b). The only difference for the simple cubic lattice is the quotient of the maximal size and average size is scaled by L^3, which is the total number of lattice sites in the system,

$$Q_{\rm sc}(p, L) = [\langle s_{\rm max}(p, L)\rangle / \langle s(p, L)\rangle]/L^3. \quad (4)$$

The data for the positions of the maximum of $Q_{\rm sc}(p, L)$ for the lattice sizes $L = 32$–256 are used to extrapolate $\langle p_{\rm max}(L)\rangle = p_{\rm max} - \text{const} \times L^{-1.812}$, with $p_{\rm max} = 0.3448$ [Fig. 11(b)].

Therefore, in each of the three lattices, namely, square, triangular, and simple cubic, we see that the precise values of the probabilities $p_{\rm max}$ are about 1% larger than their corresponding percolation thresholds p_c. Clear power laws for the finite-size extrapolations in Figs. 6 and 11 in all three cases indicate that indeed these threshold values $p_{\rm max}$ are distinct from their p_c values. These extrapolations are characterized by the exponents whose values are very close, namely, 1.041 for the square lattice and 1.053 for the triangular lattice, and widely different 1.812 for the simple cubic lattice, which may be an indication of the universality of the finite-size correction exponent. It may be that more extensive study in the future with much larger systems would yield values 1 and 2 for these exponents in two and three dimensions, a possibility which we cannot rule out at this moment. Our conclusion that the $p_{\rm max}$ are different is also been supported by the independent measurements of the average mass of the largest clusters at $p_{\rm max}(L)$, which yield that indeed these clusters are of compact structures instead of being fractals at their percolation thresholds. Here we recall another problem of percolation connectivity between two points at a distance of separation of the order of the system size [21–23]. Also, enhanced thresholds for the percolation connectivities of the modified structure have been observed.

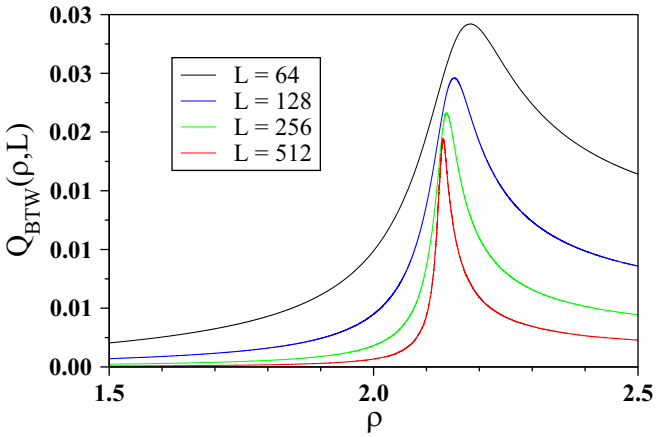

FIG. 12. For the BTW sandpile, the values of $Q_{\mathrm{BTW}}(\rho, L)$ plotted against the average number of sand particles ρ dropped per site of a square lattice.

III. BTW SANDPILE

The BTW sandpile [13] has been studied on a square lattice of size $L \times L$ with open boundary conditions. The dynamical evolution of the sandpile starts from a completely empty lattice. Sand particles are dropped one by one at randomly selected lattice sites. The system is allowed to relax through the deterministic BTW sandpile dynamics [13]. The avalanche created by dropping one particle has size s, measured by the total number of sand column topplings in the avalanche. At any arbitrary intermediate stage of the sandpile dynamics, let ρ be the average number of sand particles dropped per lattice site. We refer to it as the drop density, which is a measure of the net inward current of sand mass. This implies that an average number ρL^2 of particles have been dropped onto the system, many of which have left the system by jumping out through the boundary. Therefore, the drop density ρ of particle addition is the control variable in this problem.

We keep track of the maximal size $s_{\max}(\rho, L)$ of all the avalanches created until ρL^2 particles have been dropped. At the same time we also calculate the cumulative average size $s_{\mathrm{av}}(\rho, L)$ of all the avalanches of sizes larger than zero, including the largest avalanche. Each run consists of a sequence of particle drops until the system moves well inside the stationary regime. We check that running the simulation until the drop density reaches a value of $\rho = 2.5$ ensures arrival at the stationary state. Quantities that are averaged over many such independent runs are denoted by angular brackets. Finally, we define a Q factor, which is the quotient of the largest avalanche size and the average avalanche size of the sandpile

$$Q_{\mathrm{BTW}}(\rho, L) = [\langle s_{\max}(\rho, L)\rangle / \langle s_{\mathrm{av}}(\rho, L)\rangle]/L^2, \qquad (5)$$

and plot this quantity against the drop density ρ in Fig. 12. There is a nice peak of the value $Q_{\max}(L)$ at the position $\rho_{\max}(L)$ which we measure for four different system sizes. The rise and fall of $Q_{\mathrm{BTW}}(\rho, L)$ values on the two sides of $\rho_{\max}(L)$ are found to asymmetric. Therefore, the variation of $Q(\rho, L)$ against ρ around the drop density $\rho_{\max}(L)$ has a λ shape and the peak becomes sharper as the system size becomes larger. In the subcritical regime, the sizes of all avalanches are small, so the value of Q is small and approximately 1.

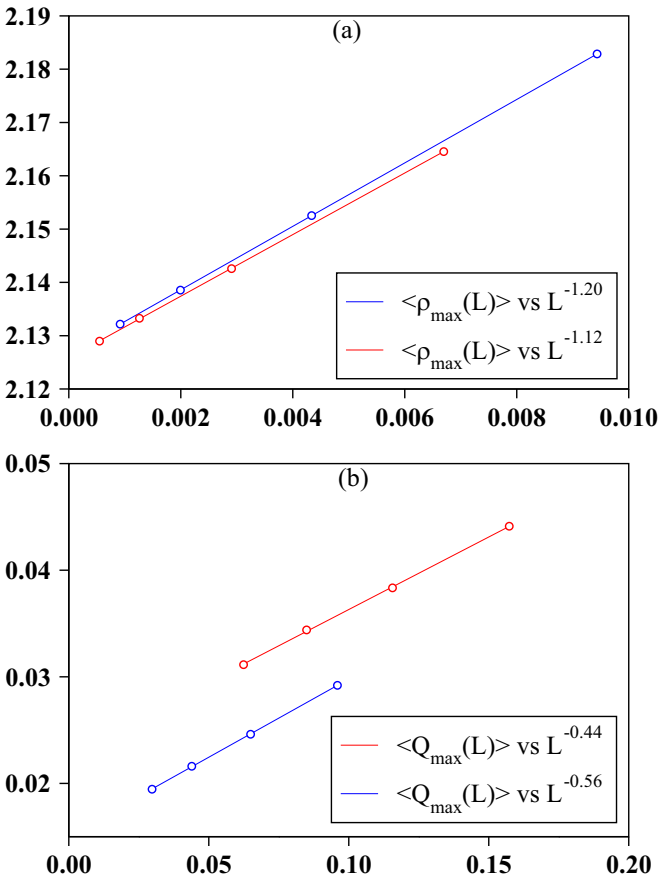

FIG. 13. For the BTW sandpile, (a) the drop densities $\langle \rho_{\max}(L)\rangle$ for the maximal Q factors and (b) the average values of the maximal Q factors $\langle Q_{\max}(L)\rangle$ plotted against different negative powers of L. The two colors, red and blue, represent two different types of calculations. The extrapolated values in the asymptotic limit of $L \to \infty$ are consistent with each other.

The moment the system moves into the stationary regime, a very large avalanche abruptly appears which is quite generic in all sandpile models. This makes the value of $s_{\max}$ in the numerator quite large, but in comparison the value of s_{av} in the denominator increases only a little since all the avalanches share this increase in the total sum of all the avalanches. This results in a rapid increase of Q. Beyond the drop density $\rho_{\max}(L)$ the system moves into the stationary state where $s_{\max}$ increases very slowly, but s_{av} increases very fast to reach a steady value. This ensures that after the peak $Q(\rho, L)$ takes a stationary value as both the numerator and denominator assume steady values. This explains the λ shape of the peak.

For a single sequence of sand grain additions on a system of size L, let $\rho_{\max}(L)$ be the precise value of the average number of particles dropped per site of the lattice corresponding to the maximum value $Q_{\max}(\rho, L)$ of the Q factor of Eq. (5). We calculate $\langle \rho_{\max}(L)\rangle$ using two different methods and plot the values against two different negative powers of L in Fig. 13(a). The red line represents the following calculation. For each run we have the maximum value $Q_{\max}(\rho, L)$ of Q and its corresponding drop density $\rho_{\max}$. These two quantities are then averaged over a large number of independent runs. It is observed that both $\langle \rho_{\max}(L)\rangle$ and $\langle Q_{\max}(\rho, L)\rangle$ depend on the system

size L [Fig. 13(b)]. The best values of the exponents for extrapolation of these two quantities are selected using the least-squares-fit method and the straight lines are then extrapolated to the $L \to \infty$ limit. We find $\langle \rho_{\max}(L) \rangle = 2.127 + 5.95L^{-1.12}$ and $\langle Q_{\max}(L) = 0.023 + 0.136L^{-0.44}$. The blue line represents the following calculation. Using a large number of runs, we calculate for each value of ρ the values of $\langle s_{\max}(\rho, L) \rangle$ and $\langle s_{\rm av}(\rho, L) \rangle$ and then calculate $Q(\rho, L)$ using Eq. (5). The maximum value $Q_{\max}(\rho, L)$ is determined and its location $\rho_{\max}(L)$ is estimated. They are again best fitted by the least-squares method and then extrapolated. We find $\langle \rho_{\max}(L) \rangle = 2.126 + 5.78L^{-1.20}$ and $\langle Q_{\max}(L) \rangle = 0.015 + 0.147L^{-0.56}$.

IV. SUMMARY

One way to answer the question of how far the topper is ahead of a typical student in a class may be by looking at the total marks obtained on the final examination. Similarly, how the richest in a society is ahead of the average members can be estimated by looking at their wealth. In addition, how the most famous research paper of a reputed scientist enjoys the maximum credit compared to the average credit of all their papers can be gauged by looking at their updated list of citation indices. Quite possibly one can cite more examples where the credit of the topper is compared with the average credit of a typical individual.

All these examples are dynamic in nature, e.g., the identification of the topper and the marks secured by them changes from one exam to the other. The identity of the richest may also change from one year to the next, as well as the citations received by the best paper of the scientist. Therefore, we thought it best to consider a so-called competition between the topper and the average and quantify this by defining the quotient of their credits as the Q factor. The natural question that comes to the mind is why this study is important at all. The reason is this factor is a quantitative measure of the fluctuations of the marks obtained by the students, the wealth possessed by different members of a society, or the quality of the papers written by the scientist.

We would like to recall that the citation statistics of the majority of scientists indicated a growth of fluctuations in citations with time. For very "successful" scientists, the statistical measures seem to indicate that these fluctuations reach a universal SOC level. It was also observed that for a successful scientist the ratio of the citation number of the highest cited paper to the average citation of all their papers often takes a value beyond a threshold (peak) value. In comparison, the value of the same ratio for not so reputed scientists does not reach that desired level.

This observation gave us the clue that the behavior of the quotient of the largest to the average credits may be interesting to study in other physical systems as well. Therefore, in this paper we decided to apply this idea to systems well known in statistical physics. One example was the problem of percolation from equilibrium systems and another was the sandpile model of self-organized criticality from nonequilibrium systems. Both systems evolved under suitably defined dynamical rules. We defined the connected clusters in the percolation process and the avalanche clusters in the sandpile model analogously to the group of members in a society. Though these systems in their early stages were uncorrelated, under the process of evolution they gradually became correlated. The signature of the correlation was traced in the rapid growth of the largest cluster in the percolation process and the largest avalanche in the sandpile model. The credits possessed by these members were estimated by the cluster sizes and the avalanche sizes.

In both examples, the system passed through a transition point. On increasing the site occupation probability, the percolating system made a transition from the subcritical phase to the supercritical phase through the critical point. At this point the size of the largest cluster grew at the fastest rate compared to the average size of all clusters. However, immediately after the percolation transition the rate of growth of the largest cluster slowed down. As a consequence, the Q factor exhibited a peak at a specific value of the site occupation probability $p_{\max}$ which was approximately 1% larger than the percolation threshold p_c of all lattices. We argued that these two numbers $p_{\max}$ and p_c cannot be the same, only because the percolation transition is a continuous transition. A very similar scenario arose for the sandpile model, where the current size of the largest avalanche underwent a large jump in its size when the system moved into the self-organized stationary state.

ACKNOWLEDGMENTS

We are very much grateful to A. Aharony and R. Ziff for their insightful comments and suggestions. B.K.C. is grateful to the Indian National Science Academy for their Senior Scientist Research Grant.

[1] H. E. Stanley, *Introduction to Phase Transitions and Critical Phenomena* (Clarendon, Oxford, 1971).
[2] P.-G. de Gennes, *Scaling Concepts in Polymer Physics* (Cornell University Press, Ithaca, 1979).
[3] D. Stauffer and A. Aharony, *Introduction to Percolation Theory* (Taylor & Francis, London, 1991).
[4] P. Bak, *How Nature Works: The Science of Self-Organized Criticality* (Copernicus, New York, 1996).
[5] V. Pareto, *Cours d'Économie Politique* (Rouge, Lausanne, 1897).
[6] M. O. Lorenz, Methods of measuring the concentration of wealth, Publ. Am. Stat. Assoc. **9**, 209 (1905).
[7] C. W. Gini, *Variabilitá e Mutabilitá: Contributo allo Studio delle Distribuzioni e delle Relazioni Statistiche* (Cuppini, Bologna, 1912).
[8] J. E. Hirsch, An index to quantify an individual's scientific research output, Proc. Natl. Acad. Sci. USA **102**, 16569 (2005).
[9] A. Ghosh, N. Chattopadhyay, and B. K. Chakrabarti, Inequality in societies, academic institutions and science journals: Gini and k-indices, Physica A **410**, 30 (2014).

[10] A. Ghosh and B. K. Chakrabarti, Limiting value of the Kolkata index for social inequality and a possible social constant, Physica A **573**, 125944 (2021).

[11] A. Ghosh and B. K. Chakrabarti, Scaling and kinetic exchange like behavior of Hirsch index and total citation distributions: Scopus-CiteScore data analysis, Physica A **626**, 129061 (2023).

[12] S. S. Manna, S. Biswas, and B. K. Chakrabarti, Near universal values of social inequality indices in self-organized critical models, Physica A **596**, 127121 (2022).

[13] P. Bak, C. Tang, and K. Wiesenfeld, Self-organized criticality: An explanation of $1/f$ noise, Phys. Rev. Lett. **59**, 381 (1987).

[14] S. S. Manna, Two-state model of self-organized criticality, J. Phys. A: Math. Gen. **24**, L363 (1991).

[15] A. Ghosh and B. K. Chakrabarti, Do successful researchers reach the self-organized critical point? Physics **6**, 46 (2024).

[16] R. I. M. Dunbar, Neocortex size as a constraint on group size in primates, J. Hum. Evol. **22**, 469 (1992).

[17] Dunbar's number, Wikipedia, https://en.wikipedia.org/wiki/Dunbar's_number.

[18] J. Hoshen and R. Kopelman, Percolation and cluster distribution. I. Cluster multiple labeling technique and critical concentration algorithm, Phys. Rev. B **14**, 3438 (1976).

[19] J. L. Jacobsen, Critical points of Potts and O(N) models from eigenvalue identities in periodic Temperley–Lieb algebras, J. Phys. A: Math. Theor. **48**, 454003 (2015).

[20] A complete list of percolation thresholds is available from Wikipedia, https://en.wikipedia.org/wiki/Percolation_threshold.

[21] S. S. Manna and R. M. Ziff, Bond percolation between k separated points on a square lattice, Phys. Rev. E **101**, 062143 (2020).

[22] W. Glänzel, On the h-index - A mathematical approach to a new measure of publication activity and citation impact, Scientometrics **67**, 315 (2006).

[23] A. Yong, Critique of Hirsch's citation index: A combinatorial Fermi problem, Not. Am. Math. Soc. **61**, 1040 (2014).